EUROPEAN ORGANIZATION FOR NUCLEAR RESEARCH

HIGH-ACCURACY, BIDIMENSIONAL READ-OUT OF PROPORTIONAL CHAMBERS WITH SHORT RESOLUTION TIMES

A. Breskin, G. Charpak, C. Demierre, S. Majewski,
E. Policarpo, F. Sauli and J.C. Santiard

CERN, Geneva, Switzerland

ABSTRACT

The pulses induced on orthogonal cathode strips are integrated after filtering through gates of variable widths, down to about 30 nsec. The determination of the charge centroid gives two coordinates. With minimum ionizing particles the accuracy along the wires is better than 200 μm (FWHM).

The advantages of the method over other read-out methods or drift chambers are discussed. The pulse-height information may permit ambiguity removal for multiple tracks.

Geneva - 20 December 1976

(Submitted to Nuclear Instruments and Methods)

1. INTRODUCTION

When an avalanche occurs on an anode wire of a multiwire proportional chamber (MWPC), there are induced positive charges on the surrounding electrodes. Cathode planes made of wires or strips provide a convenient way of measuring the induced charge distribution, which is centred on the avalanche position[1]. The full width at half maximum (FWHM) of the distribution of the induced pulses is quite large, approximately 2L, where L is the anode-cathode distance[1-4]. However, the centroid of the distribution is well defined. The first accurate measurements in a MWPC, with an analogic method, of the centroid of avalanches produced by X-rays of 5.9 keV, gave resolutions of the order of 350 μm (FWHM)[5]. Using the method of cathode-coupled delay lines, some authors[3] obtained similar resolutions for minimum ionizing particles at normal incidence. Almost all the various methods, based on delay line or charge division, give the same accuracy[6], with some features favouring particular applications.

The read-out of the pulse height induced on cathode strips and the computation of the centroid[7] have been used in several X-ray detectors developed at CERN[8,9]. This computation has been done either by digital or by analogic methods[10,11], the incentive to develop the direct computation rather than use other methods referred to above arising from the following considerations:

- the method should give the ultimate accuracy determined by the spatial distribution of charges;
- the measurements are local, in the sense that the induced pulses do not have to propagate along the whole length of the chambers.

The application of the method for the localization of minimum ionizing particles was investigated. It seems that the accuracy is better than the one of drift chambers, and that short resolution times, e.g. 30 nsec, can be used. Two-dimensional read-out of planes can be obtained with an interpolation of the track position between wires for a large fraction of incidence angles. For several tracks the possibility of ambiguity resolution arises through the use of the energy loss information. At this stage we can already foresee many cases where such a localization approach is preferable to any one available, and may justify the presentation of those preliminary results.

2. CHAMBER CONSTRUCTION

The chamber anode is a plane made of gold-plated tungsten wires, 10 μm diameter, 1 mm or 2 mm apart, sandwiched between two cathode planes. These are at a distance of 8 mm and are made of wires of 50 μm diameter, 500 μm apart. The cathode

wires are connected in groups of six wires. In one cathode plane the wires are parallel to the anode wires; in the other they are orthogonal (see Fig. 1).

The positive pulses induced on the groups of six cathode wires, which we call strips, are amplified and used for the position determination by calculation of the centroid. The anode wires are in general connected together and used only for timing or trigger purposes.

The gas filling is either the magic gas[12]: argon (70%), isobutane (29.5%), methylal (3%), and freon-13 B1 (0.5%); or the same gas but without freon.

3. ELECTRONICS

In high-energy physics, interest is usually centred around selected types of events, and it is only rarely that the coordinates of all the particles crossing a chamber are needed. It is a problem that is quite different from, for example, that of X-rays imaging, where usually it is the fastest read-out of the coordinates of all the interaction points that is required.

The methods used so far for the fast computation of the centroid require 1 to 5 μsec [10,11], and they are very unsuited to the read-out of simultaneous particles, which is a common situation in high-energy physics. We used then a different approach, selecting those pulses connected to an interesting event by strobing them through a short linear gate. Cheap amplifiers were designed which permit the use of short gates, with noise and gain characteristics suitable for the read-out of the centroid*). These characteristics are: sensitivity 250 mV/10^{-12} coulomb; noise (peak to peak) 4×10^{-15} coulomb; rise-time (10% to 90%) < 10 nsec (about 15 nsec when connected to the cathode strip); linearity ∿ 1%. Figure 2 shows the scheme of the read-out. The pulses suitably selected by the gates are fed into analog-to-digital converters (ADC), and the centroid is calculated by the computer. This method is well adapted to most problems in high-energy physics, since very often the wanted event is a complex one, requiring a large computation capacity, and the additional burden of computing the centroids may be negligible.

4. ACCURACY CALIBRATION

The only satisfactory way of measuring the accuracy would be to have several such chambers aligned in a high-energy particle beam and to fit the straight tracks through the calculated points. However, our preliminary measurements showed that the accuracy is such that unless the chambers are constructed and mounted with accuracies of the order of 10 μm, one would not be in a position to know where the errors were really coming from. While such a device is under construction it was

*) This amplifier, designed by J.C. Santiard, CERN, has been integrated by Alcatel, France.

decided to calibrate the chamber using time selection in multiwire proportional chambers to define the position of the trajectories, and to compare them with the calculated centroids.

The chamber under study is placed in a high-energy particle beam (6 GeV/c to 15 GeV/c) between the two collimating MWPCs (2 mm anode wire spacing) at 30 cm distance (Fig. 3). These chambers are aligned in such a way that their anode wires are parallel; in each chamber a wire is selected and the pulses from the two wires are sent to a coincidence circuit. The plane of the two wires is aligned on the average beam direction. The usual set of scintillators is used, providing the zero time and defining the dimension of the beams being selected in the direction of the wires of the collimating chambers. In the direction orthogonal to this one, beam widths were defined by drift time on the collimating chambers, to the two selected wires.

If the timing of the pulses from the two wires is adjusted so as to take the first arriving pulses, the zero time being given by the scintillation counters, then only those trajectories close to the wires are selected; and under this condition the FWHM of the defined beam is $\sim$ 200 μm.

To test the accuracy of the centroid measurements along the anode wires of the chamber being tested, this chamber was positioned between the two collimating chambers, with its anode wires orthogonal to the collimating wires. The variation of the centroid position as a function of the angle of the chamber relative to the beam, of the width of the ADC gate, and of the anode voltage, was then studied. To study the interpolation between wires, the same procedure was used, but with the anode wires of the chamber being tested parallel to the collimating wires.

5. PRELIMINARY MEASUREMENTS

A few preliminary measurements, essentially to get information on the intrinsic accuracy of the electronics, were made using 5.9 keV X-rays, the "magic gas", and 3.9 kV anode voltage. The X-ray beam was collimated with a 0.1 mm collimator, which, taking into account the range of the photoelectrons, gives an effective width for energy deposition in the chamber extending up to about 250 μm. Figure 4 shows the centroid distribution in the direction of the anode wires for two collimated beams at a distance of 1 mm; the FWHM is 250 μm. Owing to the straggling of the spread of the avalanches along the wire and to the effective beam width, measurements along the direction of the wires do not provide information on the intrinsic accuracy of the electronic system; on the other hand, this accuracy is to some extent calibrated by looking at the centroid distribution in the direction orthogonal to the anode wires. Such a measurement is shown in Fig. 4, the two peaks being 1 mm apart and featuring a FWHM of 60 μm. This width is still

connected to real charge-distribution fluctuations and not only to electronics. Indeed, if the collimated X-ray beam was positioned in such a way that the effective energy deposition region in the chamber was only on the left or on the right of a wire, a slightly narrower centroid distribution was observed. Also a slight displacement of the peak was detected for a right or a left irradiation of a wire.

6. ACCURACY OF THE CENTROID MEASUREMENTS ALONG THE WIRE

For beams orthogonal to the chamber, the size of the cloud of primary electrons along the wire, arising from a particle, is mainly determined by the range of primary electrons, the geometry of the local electric field, and diffusion effects. For inclined tracks one expects that a larger region of the wire is "touched" by the primary electrons owing to the projection of the track onto the wire. The next step in the building up of the space-charge distribution, whose centroid is read by the strips through the induced charges, is that of the avalanche processes. These are determined not only by the rate of arrival of the primary electrons and the extension of the region that they "touch", but also, and in the case of the magic gas in a determinant way, by space-charge saturation effects and the spread of the avalanches. Even with a magic gas, for inclined tracks, it can be expected that electrons arriving later and further away from the region of arrival of the first ones, may be independently amplified, thus contributing also to the pulse lengthening.

These qualitative remarks agree with the experimental observations. Indeed for orthogonal beams the strip pulses were $\sim$ 50 nsec wide, while they were about 100 nsec wide with the chamber inclined 31° in respect to the beam (see Fig. 5). In this figure a gate pulse of 30 nsec and with zero delay relative to the strip pulse is also shown.

It is then clear that the FWHM of the centroid as measured by the strip pulses will depend on the width of the gate and on its delay relative to the initialization of the avalanches, for a beam of a certain width. This is a physical effect that has nothing to do with the behaviour of the electronic system: for too short gates or too large delay times, one simply expects bad signal-to-noise ratios, as the amount of charge integrated by the ADCs while the gate is opened is smaller, with a consequent broadening of the centroid of the distribution. Indeed it was found that, for a gate width of 50 nsec with zero delay time, the FWHM of the centroid distribution at 3.9 kV anode voltage is about 40% of its value at 3.7 kV; and it improves still further to about 30% at 4.1 kV, no significant improvements being observed for higher anode voltages. At 0° incidence it can be expected that, apart from electronic effects, the gate width will not play an important role on the FWHM of the centroid distributions.

Indeed with zero delay time and gates of 30, 50, and 80 nsec, no significant change was observed. For a shorter gate of 15 nsec the FWHM increased by a factor of 2, this being probably an electronic effect. Similar behaviour was observed at an angle of 20°; but at 33°, while gates of 30 nsec and 50 nsec with 0 nsec delay give similar FWHM, a gate of 50 nsec delayed by 50 nsec implied an increase of the FWHM by a factor of about 3! Also, from Fig. 5, it seems that this is not a signal-to-noise ratio effect, as the charge integrated between 50 and 100 nsec is not very different from the charge between 0 and 50 nsec, but it is related to the arrival of later electrons, far away from the mean of the centroid distribution.

A great advantage of using narrow gates is to limit the influence of the remote electrons -- of course in a much more definite way than that provided, to some extent, by the use of freon -- which contribute to reducing the accuracy in all ungated methods, e.g. delay lines or current division.

For a normal beam incidence, Fig. 6 shows the peak in the centroid distribution along the wires of the chamber under study corresponding to trajectories close to the collimating wires. The gate width was 50 nsec, without delay, and it features a FWHM of 215 μm. As noted before, 30 nsec gates give similar FWHM.

We expected a width of about 200 μm from the collimating method itself. But, as in the dimension orthogonal to the chamber wires being tested the beam width is defined by scintillators and corresponds to about 30 wires spaced at 1 mm, a deviation of less than 1% of the orthogonality between the chamber wires and the beam plane -- the wire plane still being normal to the beam plane -- would account for part of the additional broadening experimentally observed.

At inclined incidence angles, the experimentally observed FWHM were larger, and increased with the inclination but they could in the same way be accounted for by the effective beam width increase due to inclination and the same deviation from orthogonality. In other words, within experimental conditions, no broadening of the beam introduced by the read-out method could be detected.

7. INTERPOLATION BETWEEN WIRES

When the charge is split among several wires, for inclined tracks at suitable angles, the average division of charges should be done in accordance with the position of the trajectory between the wires. More specifically (Fig. 7), if the angle of incidence is such that any trajectory crosses one symmetry plane between two wires, with length L_1 and L_2 in the two respective sensitive cells, the read-out method used would, in a first approximation, give a linear interpolation if the energy losses would be proportional to L_1 and L_2 and if the charge gains were linear and equal in both wires. Because of the different arrival times of the

electrons at the two wires, even if these conditions are fulfilled, the centroid of the charge distribution as measured on the strips would be time-dependent and thus a function of the gate width. This is a second-order limitation, as the difference of arrival times can be much smaller than the gate width, the important one being that the energy losses are not proportional to L_1 and L_2 (as is well known the energy loss spectra are rather broad) nor are the charge gains the same in both wires. An extreme limit of this last situation occurs under conditions of magic gas operation, where charge saturation appears. Then, perfect saturation and similar drift times would result in a narrow peak centred between the two wires for all trajectories crossing the symmetry plane between these two wires.

Neglecting the range of primary electrons and field distortions, the energy sharing occurs for all trajectories, at a given position x from a wire, for angles greater than $tg^{-1}\left[s/2 - x)/L\right]$, where L is the effective half thickness of the chamber determined either by the gas (for electronegative attachment) or by the gate width. In our case, where gate widths of 30 or 50 nsec were aimed at, corresponding to thicknesses of 1.5 to 2.5 mm, the critical angle is rather large as it is difficult to reduce the wire spacing below 1 mm. However, it is clear that a gain in accuracy can still be expected by interpolation, even at relatively small angles, below the critical angle. The next figures illustrate some of the above statements and summarize our main results.

Figure 8 shows the centroid distribution for a uniform irradiation of the chamber at different incidence angles, using the magic gas mixture, the distance between wires being 1 mm: Fig. 8a for normal incidence; Fig. 8b for 10° incidence; and Fig. 8c for 45° incidence. We see that already at 10°, when a gate of 50 nsec was used, a notable fraction ($\sim$ 50%) of the particles gave rise to energy sharing and interpolation. They correspond to the broad bumps between wires, which in the limit of perfect charge saturation would appear as sharp lines between the peaks corresponding to the wires. Figure 8c shows that at 45° incidence, and again using a 50 nsec gate, essentially all trajectories are interpolated between wires, the uniformity of irradiation being apparent.

With a 200 μm beam defined by the collimating wires of C_1 and C_2 (see Fig. 2), Figs. 9a and 9b show the centroid distributions for several distances of the beam to a wire on the chamber under test, measured in the direction orthogonal to the beam (indicated in μm) for incident angles of 10° and 45°, respectively. The data were obtained with magic gas, and the wire spacing was 1 mm. The gates used were 50 nsec and 30 nsec, respectively, without delay. A clear difference in the shape of the centroid distributions as one goes away from a wire is seen from Figs. 9a and 9b. This is because the percentage of beam particles that is interpolated between wires in the case of Fig. 9a, at 10°, is a function of the beam position, while in the case of Fig. 9b, at 45°, there is interpolation for all particles.

By moving the chamber under test relative to a beam defined by the collimating wires, the relation between centroid positions and real positions of the beam could be measured and are shown in Fig. 10a for 35° incidence and a 30 nsec gate, and in Fig. 10b for 45° incidence and a 50 nsec gate, still using magic gas and 1 mm wire spacing. The same relation is shown in Fig. 11, but without freon, with a 100 nsec gate at 16° incidence, with a wire spacing of 2 mm, and a half thickness of 4 mm. In all these figures the real position indicated is measured in a direction orthogonal to the beam.

Referring to conditions corresponding to those of Fig. 11, it is interesting to note that even with such a thick chamber, at a relatively small angle, the accuracy was good enough to assert, within at least one-half wire spacing, where the particle crossed the chamber. This should be compared[13] with a similar result where the interpolation is obtained between two wires for tracks inclined at a given angle; indeed by selecting the events where only one wire or two wires are touched, a factor of two is gained in accuracy. But this could be done only for a given angle, while here the interpolation is continuous for angles above a critical value.

8. SPREAD OF INDUCED CHARGES AND MULTIPARTICLE SEPARATION

The sharing of charges induced by positive ions between the cathode strips has been calculated with simplifying hypotheses. Either it is assumed that one can neglect the charge image of the positive ions on the anode wires[2], or the anode wire plane is replaced by a continuous conductor[4].

Let us consider a plane cathode and orthogonal axes X and Y with origin on the intersection, with this plane, of its normal that goes through the avalanche. With the simplifying assumption that the distance travelled by the positive ions during the first tens of nanoseconds after the avalanche starts is negligible, Fig. 12 shows the relative density of charge, integrated over Y, as a function of X/L (L is the half thickness of the chamber), for the hypothesis considered above.

It was verified that the distributions of charge among strips that were observed experimentally imply a charge distribution that would lie between curves I and II of Fig. 12, as would be expected, as they correspond to extreme limits of no shielding or complete shielding by the anode wire plane. A few examples are shown in Fig. 13, where the distribution of induced charges among neighbouring cathode strips is displayed for several event positions.

A very important feature of the computed centroid method is that the information concerning the position is not only contained in the centre of gravity position but also in the shape of the charge distribution. This stability of the

charge distribution shape is best illustrated by the work of Ref. 14, where the position of the avalanche along a wire was determined by the ratio of the charges induced on two cathode strips. An accuracy of 350 μm (FWHM) was thus obtained in the avalanche position along an anode wire, illustrating the strict correlation of the charges induced in neighbouring wires. A striking example is shown in Fig. 14 where charge distributions arising from two simultaneous events are shown. But even if the two simultaneous tracks are separated by a distance too small to give two distinct peaks, the charge distribution corresponding to their centroid can be quite different from the one corresponding to a single track located at their centroid. The problem is then essentially a technique of pattern recognition.

If the distances between simultaneous particles are such that two sets of X and Y coordinates are obtained by the computer, the problem arises of associating X and Y coordinates with a certain particle. To a certain extent this problem of ambiguity is solved if a strong correlation exists between the total charge induced in the X plane, E_X, and the total charge induced in the Y plane, E_Y, for a certain particle crossing the chamber, as the X and Y coordinates of this particle are derived from the same charge induced on the strips as the corresponding E_X and E_Y information. Here the effect of screening by the anode wires may play an important role owing to the large straggling of energy losses on the two sides of the chamber, which can render this method of ambiguity solving less effective.

A few measurements were made using a β source of ^{109}Ru and two scintillators of 1×1 cm^2 to provide a trigger signal; the chamber under test had no freon, the anode wire spacing being 2 mm. In this way minimum ionizing electrons are selected. A coincidence with the scintillators' signal could also be made with the anode pulse, read by a fast preamplifier, the integrated charge pulse E_A being provided by an ADC.

For small gate widths (40 and 80 nsec) the relative standard deviation of $(E_X + E_Y)/E_A$ was about 4% if a coincidence with the anode pulse was imposed, and about 5% if the gate was opened only by the scintillators. This arises from drift time in the chamber plus the fact that the anode pulse shape is different from strip pulse shapes, as different amplifiers are used for the anode and strip signals. For larger gate widths (120 and 150 nsec), naturally the effect of making the coincidence with the anode pulse is not important and no significant variation of the relative standard deviation is observed. Concerning correlations between E_X and E_Y, the relative standard deviation of E_X/E_Y was measured for several gate widths. For any gate width between 40 and 150 nsec no important variation of the relative standard deviation is observed associated with opening the gate with only the scintillators, or with those and the anode pulse, as all strips have identical amplifiers. For gate widths of 80, 120, and 150 nsec, the relative standard deviation of E_X/E_Y was 5%, being 9% for a 40 nsec gate. Although it is possible that

noise may contribute to the decrease of the correlation between E_X and E_Y for such a short gate, a genuine shielding effect is also probably involved. If one takes the relative standard deviation of E_X/E_Y as 5%, as observed for gates of 80 nsec or larger, then Fig. 15 shows a measure of the ambiguity resolving power of the method. In Fig. 15a a measured energy distribution for relativistic particles is shown. In Fig. 15b, for this energy distribution the ambiguity resolving power R, as a percentage, is plotted as a function of the energy dissipated in the chamber. At this stage, simply as a useful criterion for defining R, the following was used: R for a certain energy loss E is the ratio of the number of events outside the range (E - 0.1E, E + 0.1E) to the total number of events. Taking into account the energy distribution, the weighted mean value of R is about 80%, a non-negligible ambiguity resolving power. Of course these are preliminary results; for example, it can be expected that the screening effect of an anode wire will depend strongly on the distance of the particle track to the wire for short distances. No measurements were done taking this parameter into account, and the correlations studied with electrons were done for broad beams. Nevertheless, these first results show that further work in this field would be worth while. The effect of high rates on the behaviour of the system was checked. As was expected, space charge build-up is its intrinsic limitation.

9. DISCUSSION OF THE RESULTS

These measurements show that the calculation of the centroid of the avalanche offers many attractive aspects:

- The time resolution can be 30 nsec for 1 mm wire spacing. It then increases with wire spacing, as in any other method, to incorporate the maximum time jitter of the pulses (of course, if the anode pulse is not used to trigger the gates of the ADC).
- The accuracy along the wire is better than 200 μm (FWHM) for normal trajectories.
- The accuracy along the wire is still better than 200 μm at incident angles up to 45°.
- The accuracy in the direction perpendicular to the wires is better than the wire spacing, except for a narrow angular range depending on the chamber thickness or the gate width. In any case, whether the chamber interpolates or not between two wires, an additional piece of information is available -- either position or angle -- which can be useful for pattern recognition.
- The pulse height is obtained for each trajectory. In the case of many simultaneous tracks, this permits to some extent the removal of ambiguities, since a large avalanche gives a large pulse height on both cathodes.

- The anode wires not being used for the coordinate measurements are available for other tasks. If they are oriented to a different direction from the cathodes they give another piece of information for ambiguity removal.

10. APPLICATIONS

The applications of the method are connected to the easiness of its implementation and its accuracy. For an equal cost it is more attractive, in most cases, than a MWPC with wire-per-wire read-out, or than a drift chamber.

The amplifiers adapted to the method are inexpensive. The pulses have to be delayed to permit decision-making to control the gate, and the most natural way is to use cables. Considerable experience exists in this field since this is still the method used by many groups to provide delays of several hundred nanoseconds wire-per-wire. For small systems this plays a small role in the cost; for large systems the fact that the delay is provided to a strip larger than the wire spacing and not to a wire makes it a reasonably small economic burden.

The pulse-height digitization is the economic bottleneck. The existing converters are usually too good and too expensive. Eight bits and 1% linearity would cover most of the needs. A cost of 20 to 40 dollars seems a reasonable value for large-scale integration of such converters, and this would reduce the cost per millimetre of chamber to values comparable to those of other methods, with the addition of considerable advantages.

In multiwire drift chambers with uniform cathode potentials, the use of orthogonal strips for the centroid determination along the wire would give planes or cylinders with about equal accuracy in all directions.

For very large chambers, where drift chambers were so far the ideal solution as far as cost and accuracy are concerned, these chambers could compete or be a useful complement. With larger gaps of, say, 1.5 cm, strips of 1.5 cm could be used. With accuracies of the order of 1 mm, a small number of relatively cheap circuits could be used for a large surface; also the delay could, in this case, be obtained from the drift in the gas itself. The resulting loss of time resolution is sometimes not a problem for very large chambers used, for instance, in high-energy neutrino experiments.

REFERENCES

1) G. Charpak, D. Rahm and H. Steiner, Nuclear Instrum. Methods 80, 13 (1970).

2) G. Fischer and J. Plch, Nuclear Instrum. Methods 100, 515 (1972).

3) J.L. Lacy and R.S. Lindsey, Nuclear Instrum. Methods 119, 483 (1974).

4) D.M. Lee, S.E. Sobottka and H.A. Thiessen, Nuclear Instrum. Methods 104, 179 (1972).

5) R. Grove, K. Lee, V. Perez-Mendez and J. Sperinde, Nuclear Instrum. Methods 89, 257 (1970).

6) V. Radeka, IEEE Trans. Nuclear Sci. NS21, No. 1, 51 (1974).

7) G. Charpak, A. Jeavons, F. Sauli and R. Stubbs, CERN 73-11 (1973).

8) G. Charpak, Z. Hajduk, A. Jeavons, R. Stubbs and R. Kahn, Nuclear Instrum. Methods 122, 307 (1974).

9) A. Jeavons, G. Charpak and R. Stubbs, Nuclear Instrum. Methods 124, 491 (1975).

10) C. Demierre and G. Vuilleumier, Proc. 2nd Ispra Symposium on Nuclear Electronics, Stresa, 1975 (EUR 5370e, EURATOM, Luxemburg, 1975), p. 151.

11) A. Jeavons, N. Ford, B. Lindberg, C. Parkman and Z. Hajduk, IEEE Trans. Nuclear Sci. NS23, No. 1, 259 (1976).

12) R. Bouclier, G. Charpak, Z. Dimčovski, G. Fischer, F. Sauli, G. Coignet and G. Flügge, Nuclear Instrum. Methods 88, 149 (1970).

13) E.A. Damaskinsky, A.P. Kashchuk, A.G. Krivshich and A.A. Vorobyov, Nuclear Instrum. Methods 130, 611 (1975).

14) G. Charpak and F. Sauli, Nuclear Instrum. Methods 113, 381 (1973).

Figure captions

Fig. 1 : Principle of the avalanche centre-of-gravity read-out method. The avalanches surrounding a wire induce a positive pulse on the cathode strips. The pulse height of the induced pulse is measured and stored, and the centre of gravity of the pulse-height distribution is computed and gives the position of the avalanche. The two cathode planes are equipped with strips parallel and orthogonal to the wires; coordinate x parallel to the sense wires, coordinate y orthogonal to the wires.

Fig. 2 : The pulses from the strips are amplified, delayed, and strobed into an analog-to-digital converter. A fast charge preamplifier had been used giving narrow pulses (typical width around 50 nsec FWHM).

Fig. 3 : Accuracy calibration. The chamber under study, C_3, shown with the anode wires vertical or horizontal, is placed between two proportional chambers, C_1 and C_2. The time interval τ, between the passage of a particle and the detection of a pulse, determines the central position of a narrow beam, with a width determined by $\Delta\tau$.

Fig. 4 : Centroid distributions with 5.6 keV X-rays.
a) Direction parallel to the wires. Two beams, collimation 0.1 mm; FWHM $\sim$ 250 µm.
b) Direction perpendicular to the wires; 1 mm wire spacing; FWHM $\sim$ 60 µm.

Fig. 5 : Pulse shapes and gating for relativistic particles. 31° incidence (20 nsec/division). Pulses induced on a cathode strip. Magic gas; 1 mm wire spacing; 4 mm gap L; 4100 V.

Fig. 6 : Centroid distribution along wires. Minimum ionizing particles; gate width 50 nsec without delay.

Fig. 7 : Interpolation between wires. If the trajectory crosses the sensitive regions of two or more wires, interpolation occurs, function of the energy losses in L_1 and L_2.

Fig. 8 : Centroid distribution in the direction orthogonal to the wires. Uniform irradiation: 1 wire/mm.
Incident angles: a) 0°; b) 10°; c) 45°. Notice the difference in the horizontal scales.

Fig. 9 : Interpolation between wires. Response to a beam of 200 µm width for different positions of the beam, measured on the direction orthogonal to the beam, indicated in µm. The number between parentheses is the

channel number corresponding to the highest channel content. The scale is 61 channels/mm for Fig. 9a and 31 channels/mm for Fig. 9b. Magic gas; 1 mm wire spacing. Incident angles: a) 10°; b) 45°.

Fig. 10 : Interpolation between wires. Response to a beam of 200 μm width for different positions. Relation between centroid positions and real position. Magic gas; 1 mm wire spacing. Incident angles: a) 35°; b) 45°.

Fig. 11 : Interpolation between wires at 16° incidence, without freon. Relation between centroid positions and real position.

Fig. 12 : Density of charge in the direction orthogonal to the cathode strips.
I) Curve predicted in Ref. 2.
II) Curve predicted in Ref. 4.

Fig. 13 : Charge distribution among cathode strips.
Strips of 3 mm; gap L = 4 mm. Experimentally measured distributions of the charges induced on neighbouring strips for various positions of the avalanches inside a strip. The distributions shape is stable for a given position.

Fig. 14 : Charge distribution for simultaneous events.
Two events separated by 1.5 cm.
Centroid position in units of strip width 3 mm.

Fig. 15 : Energy information.
a) Pulse-height distribution.
b) Ambiguity resolving power.

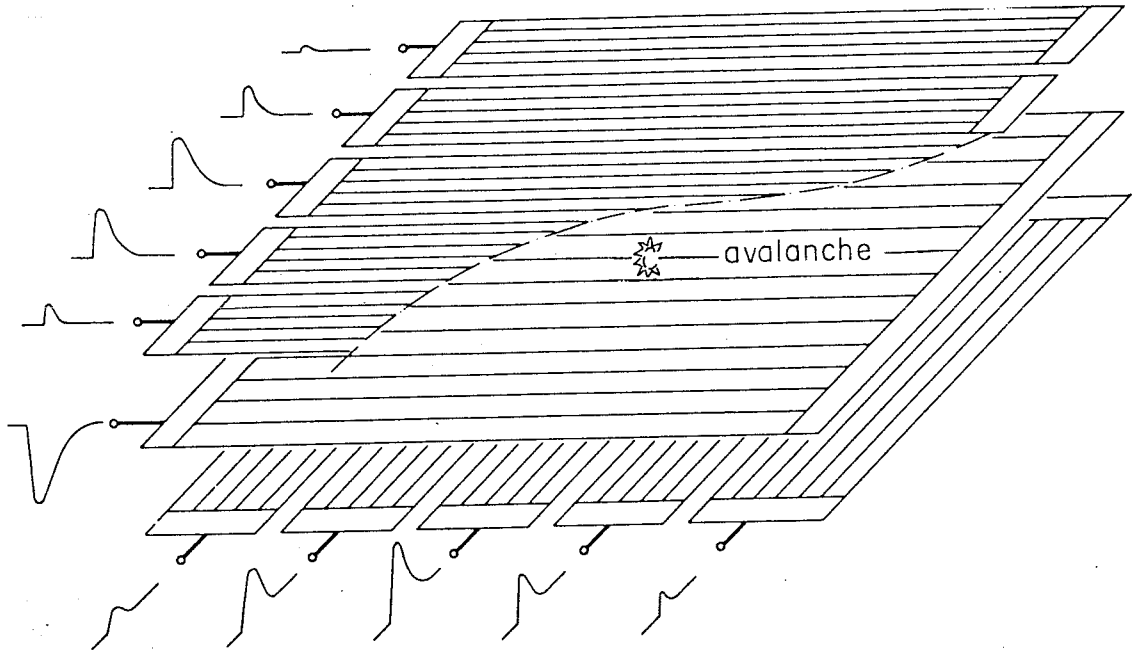

Fig. 1

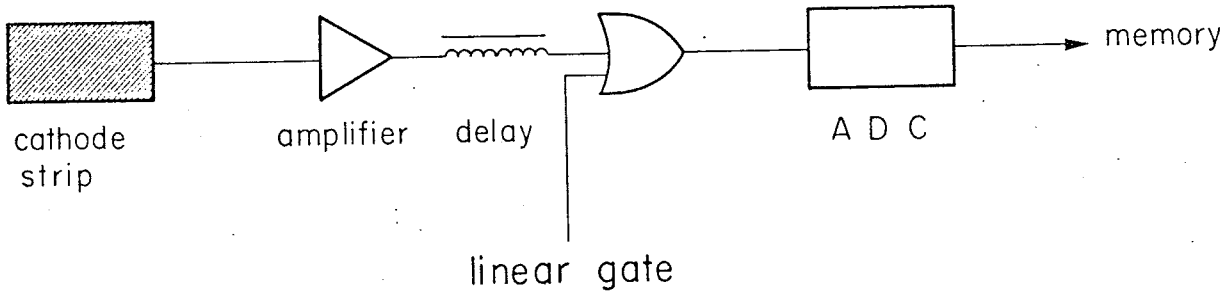

Fig. 2

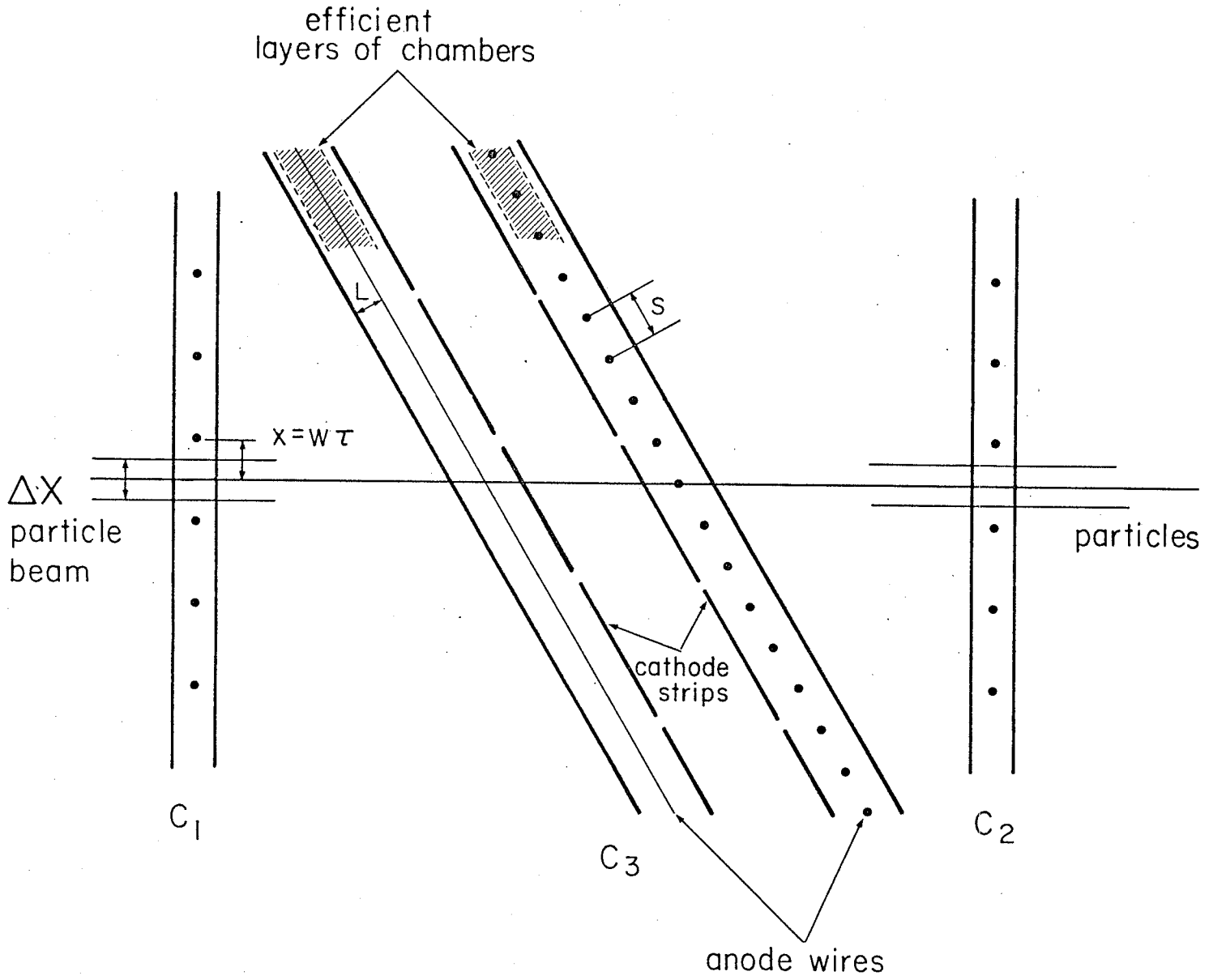

Fig. 3

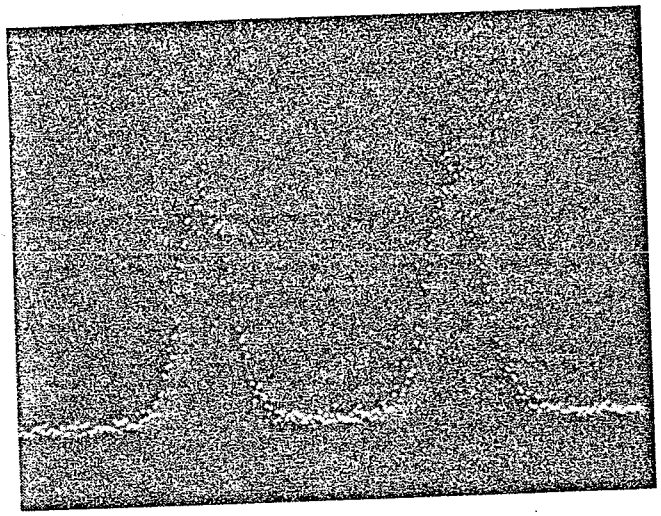

a)

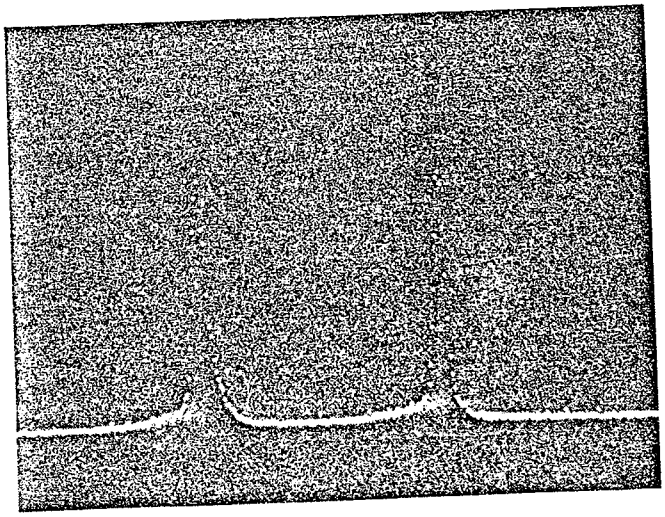

b)

Fig. 4

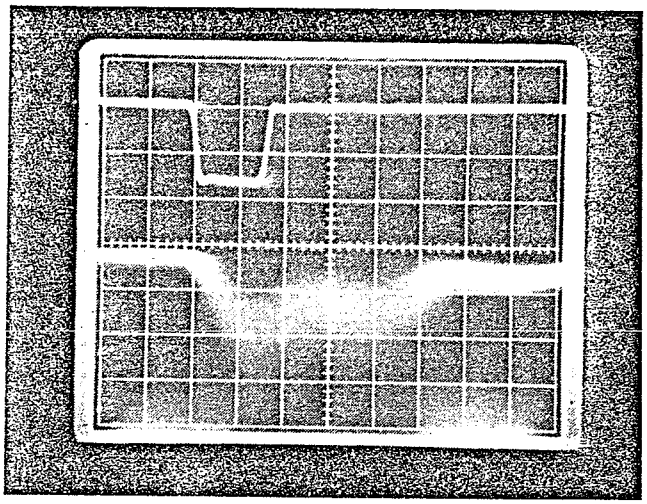

Fig. 5

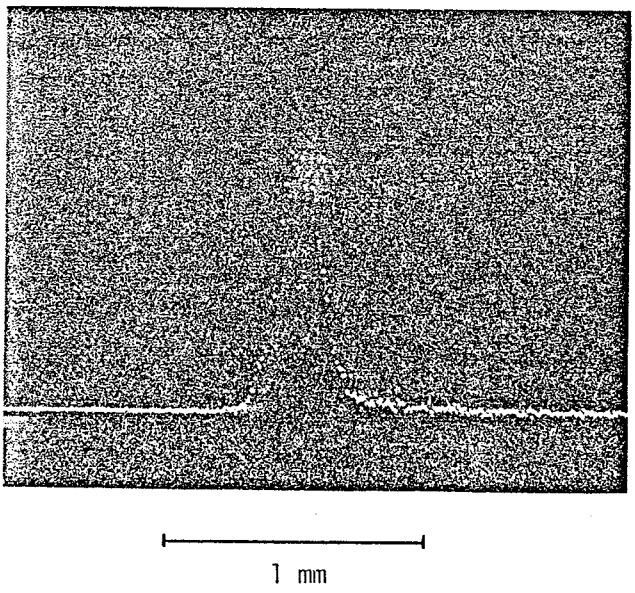

Fig. 6

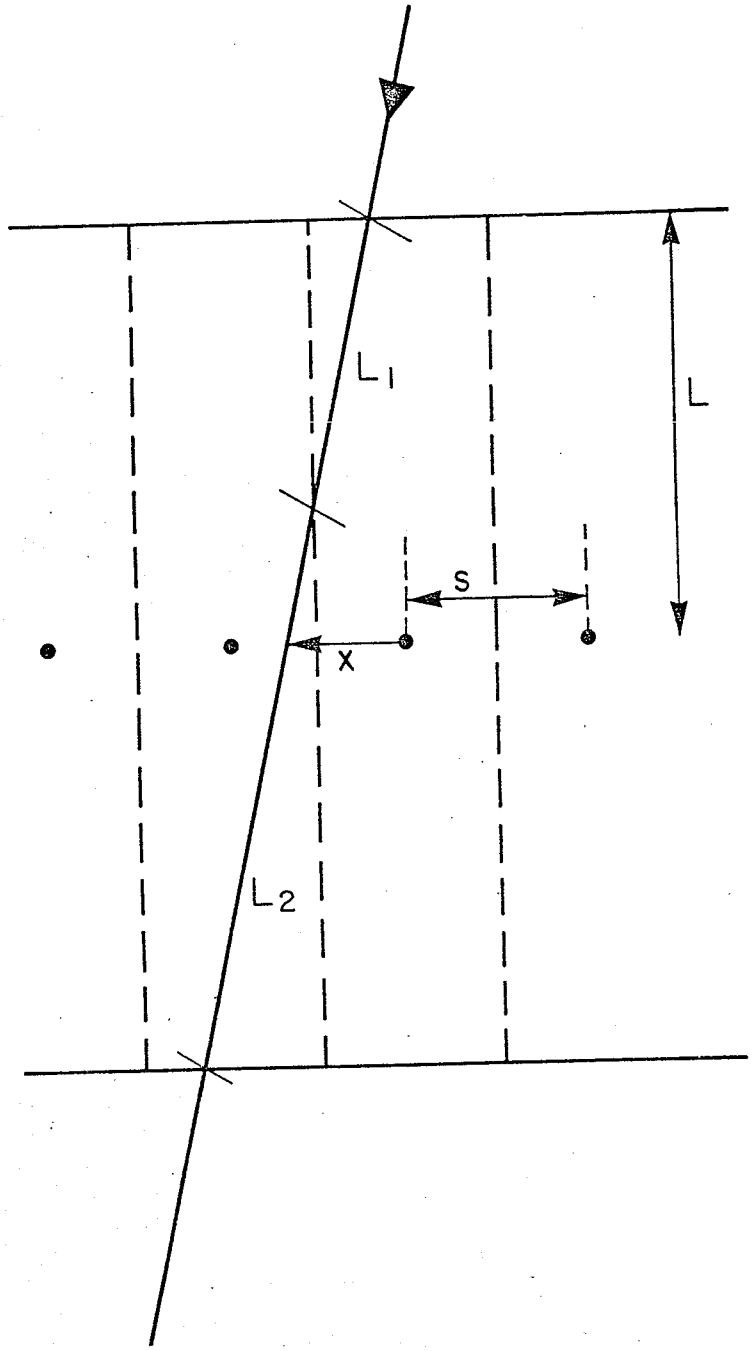

Fig. 7

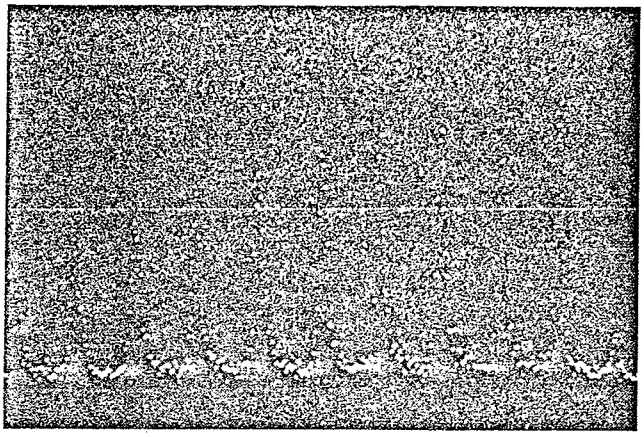

Fig. 8

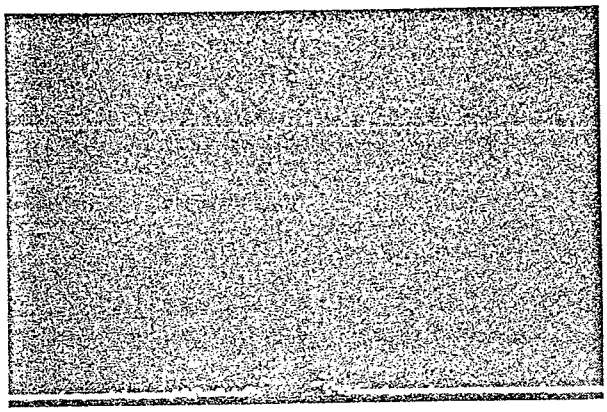

0 μm
(275)

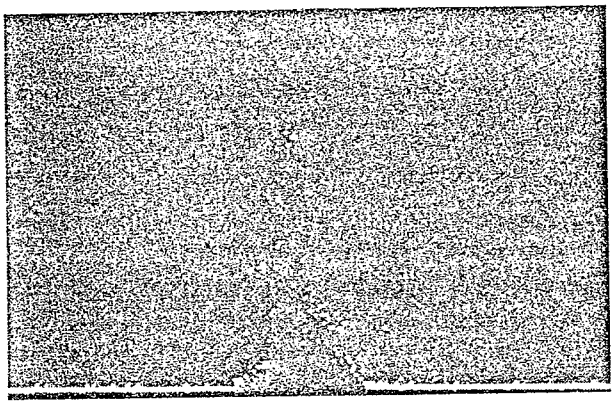

110 μm
(273)

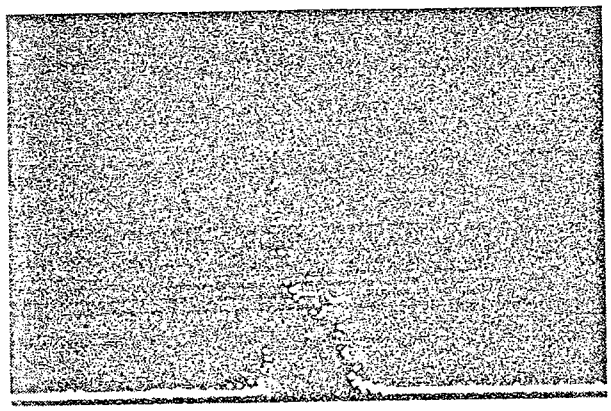

200 μm
(270)

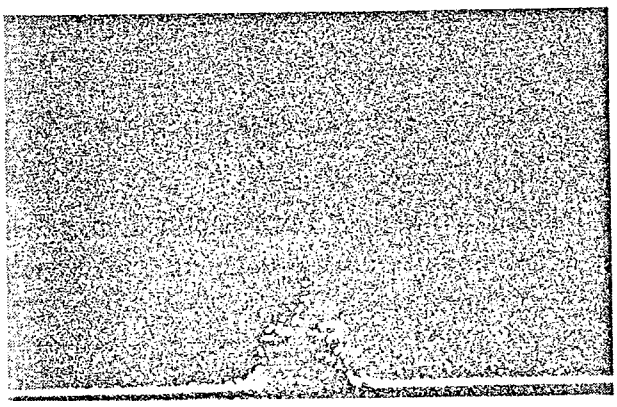

295 μm
(289)

Fig. 9a

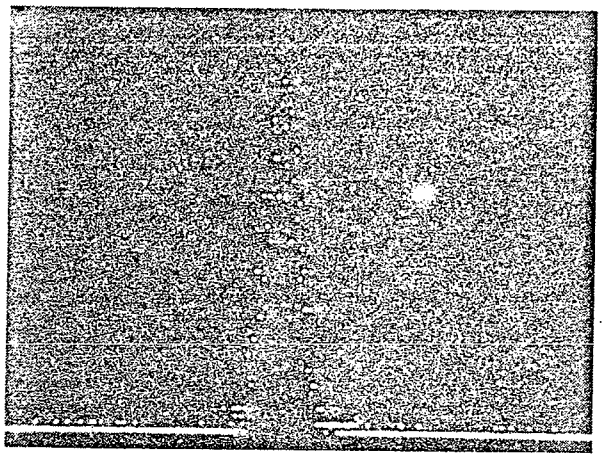

0 μm
(756)

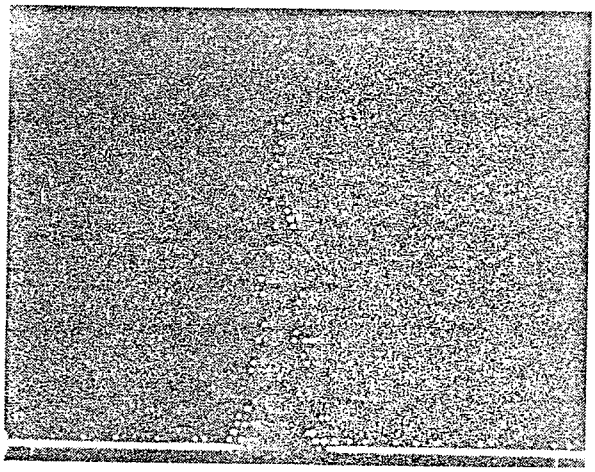

230 μm
(746)

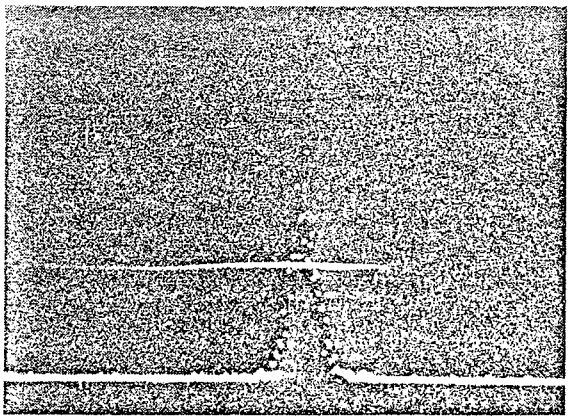

410 μm
(739)

Fig. 9b

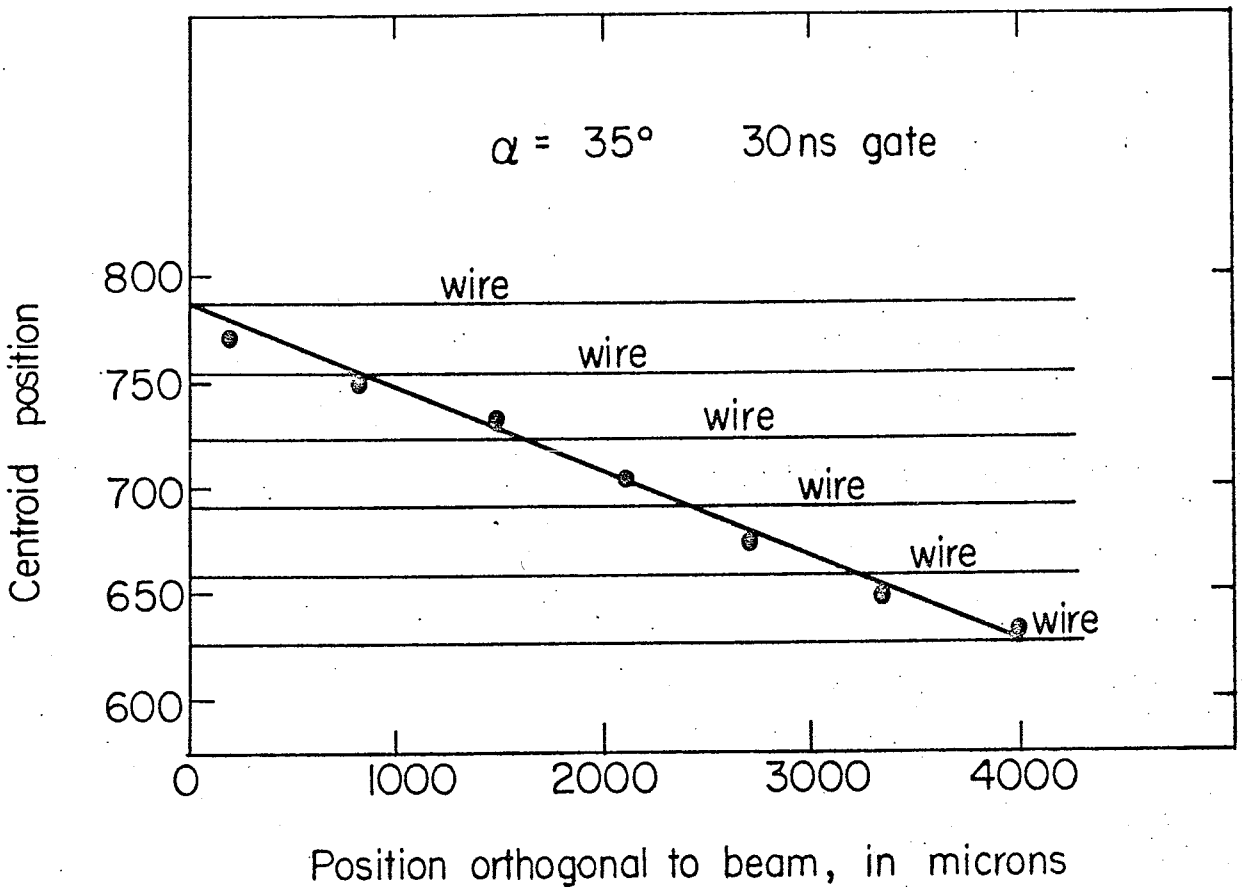

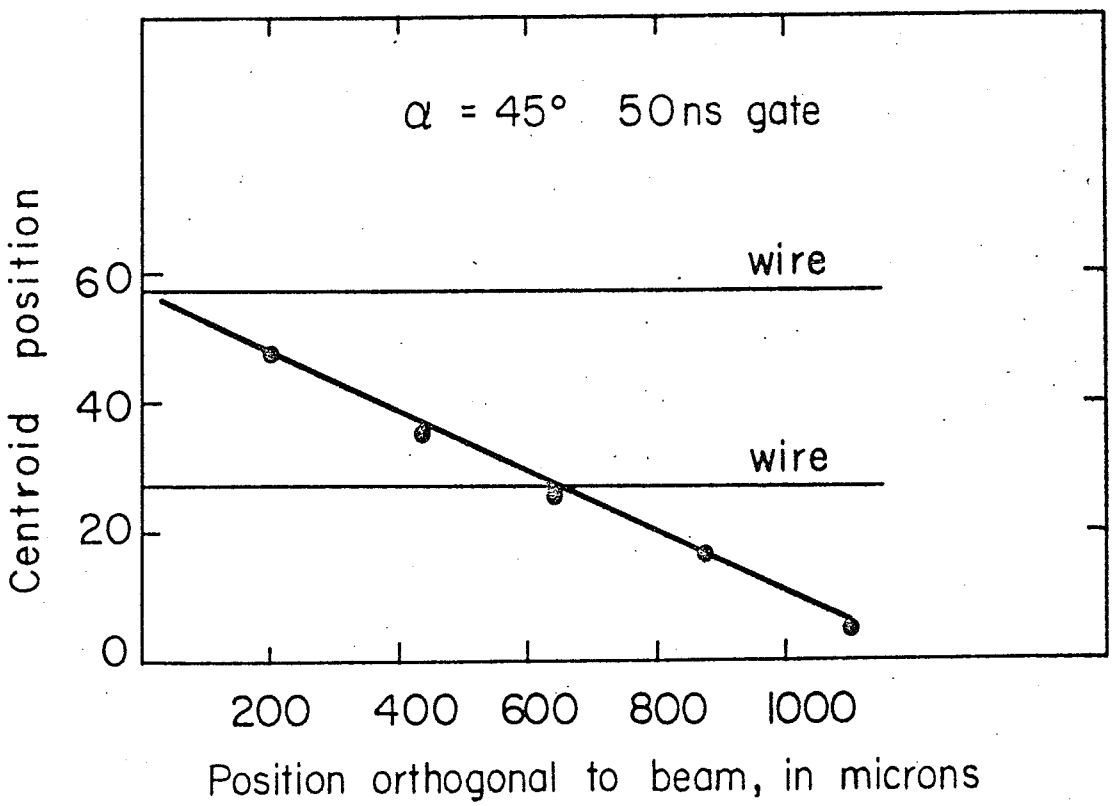

Fig. 10

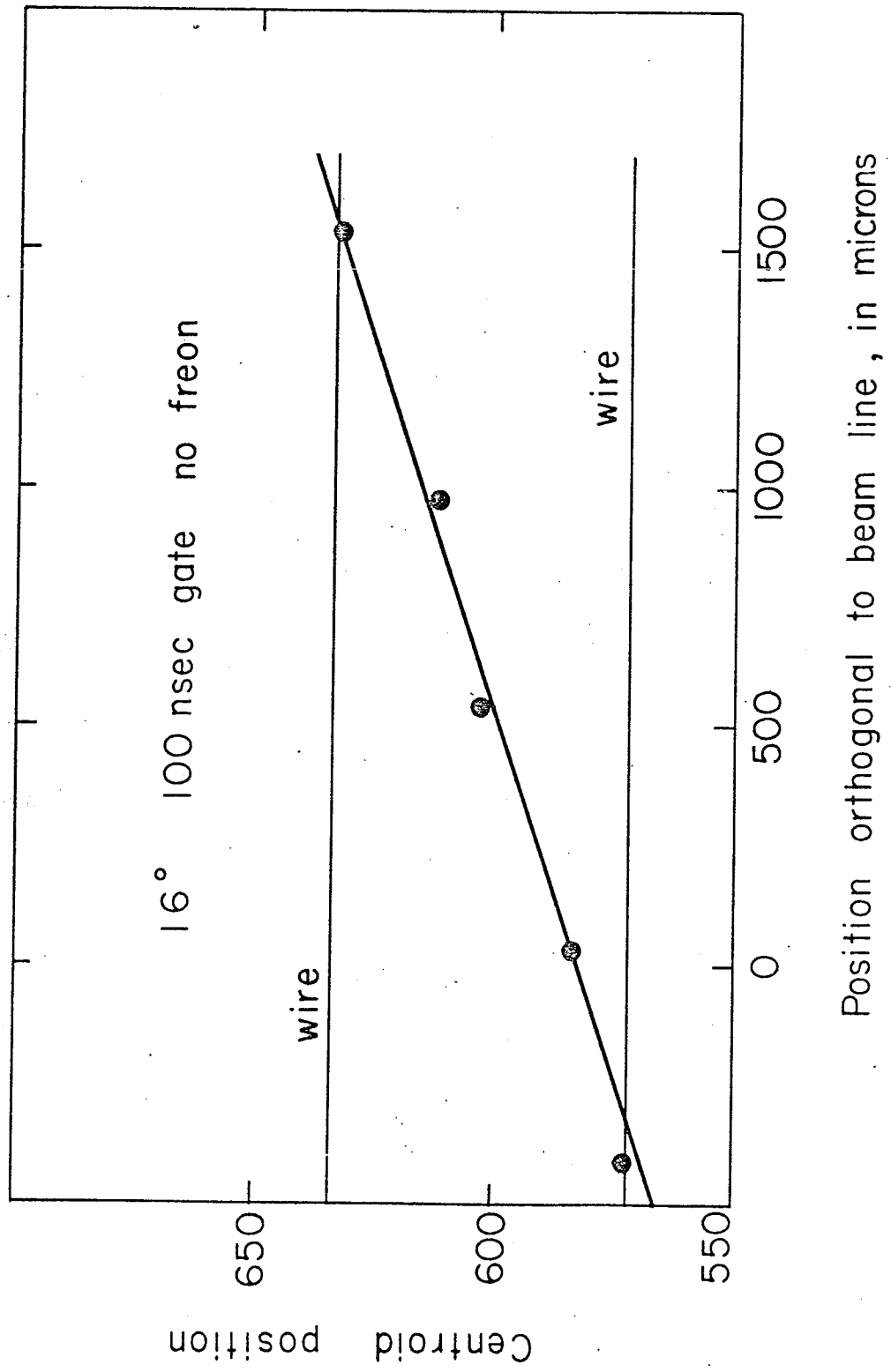

Fig. 11

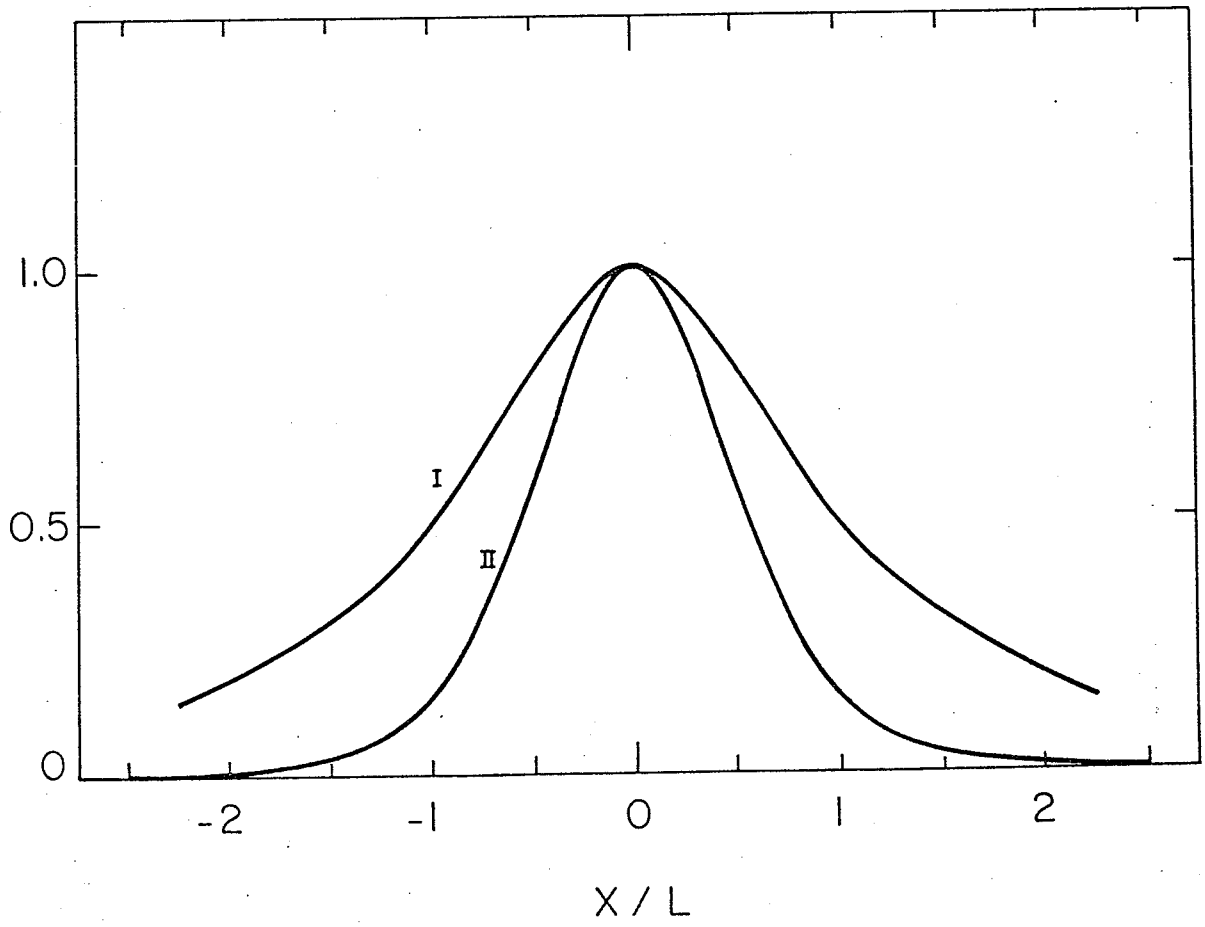

Fig. 12

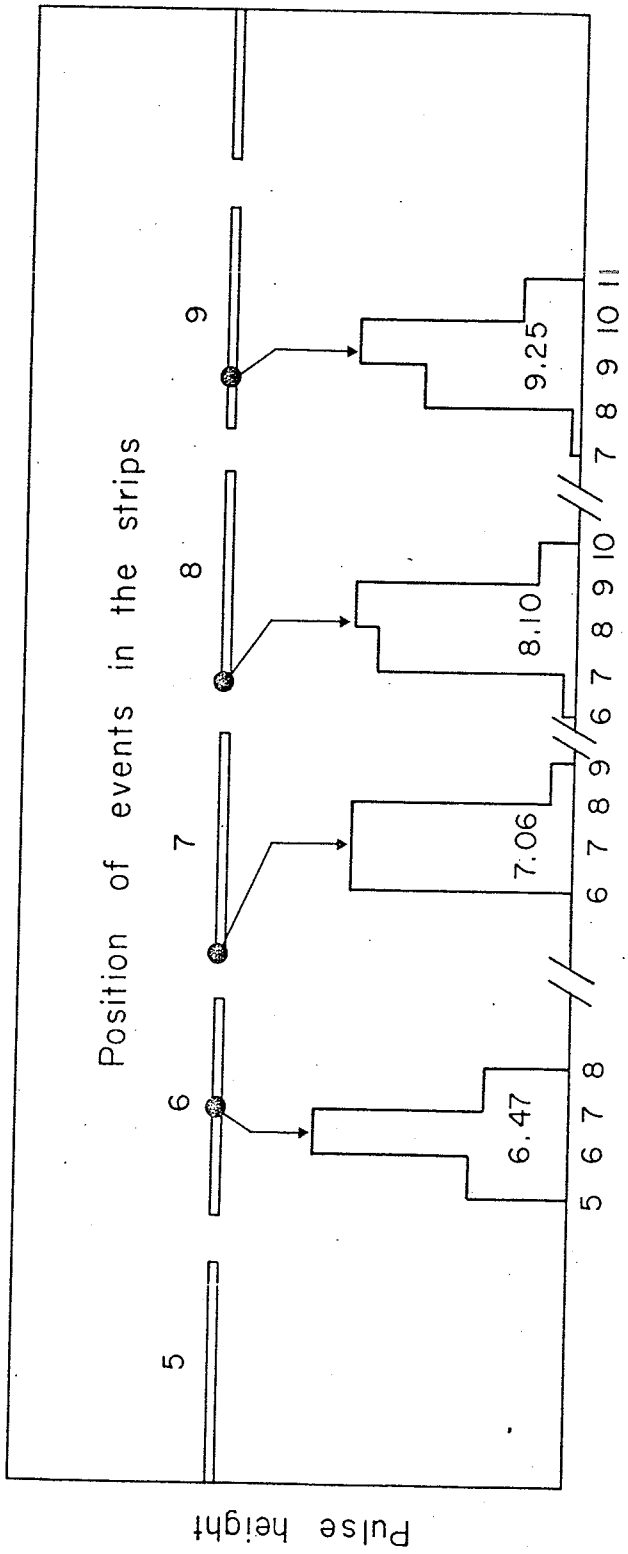

Fig. 13

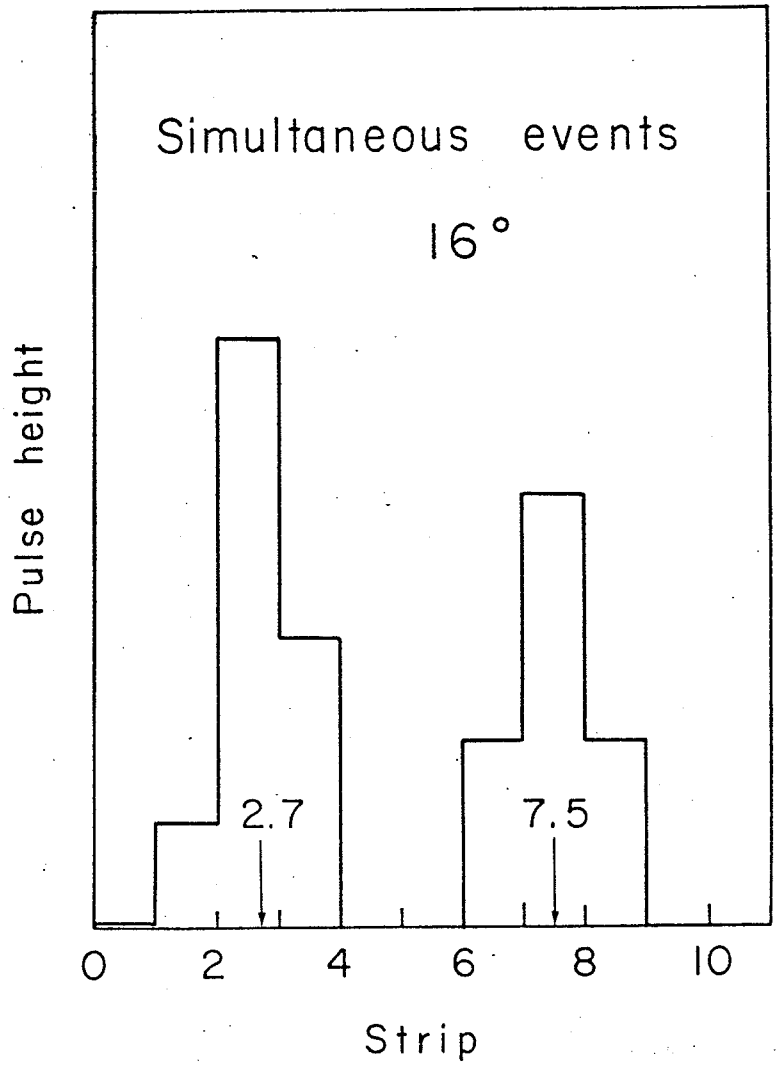

Fig. 14

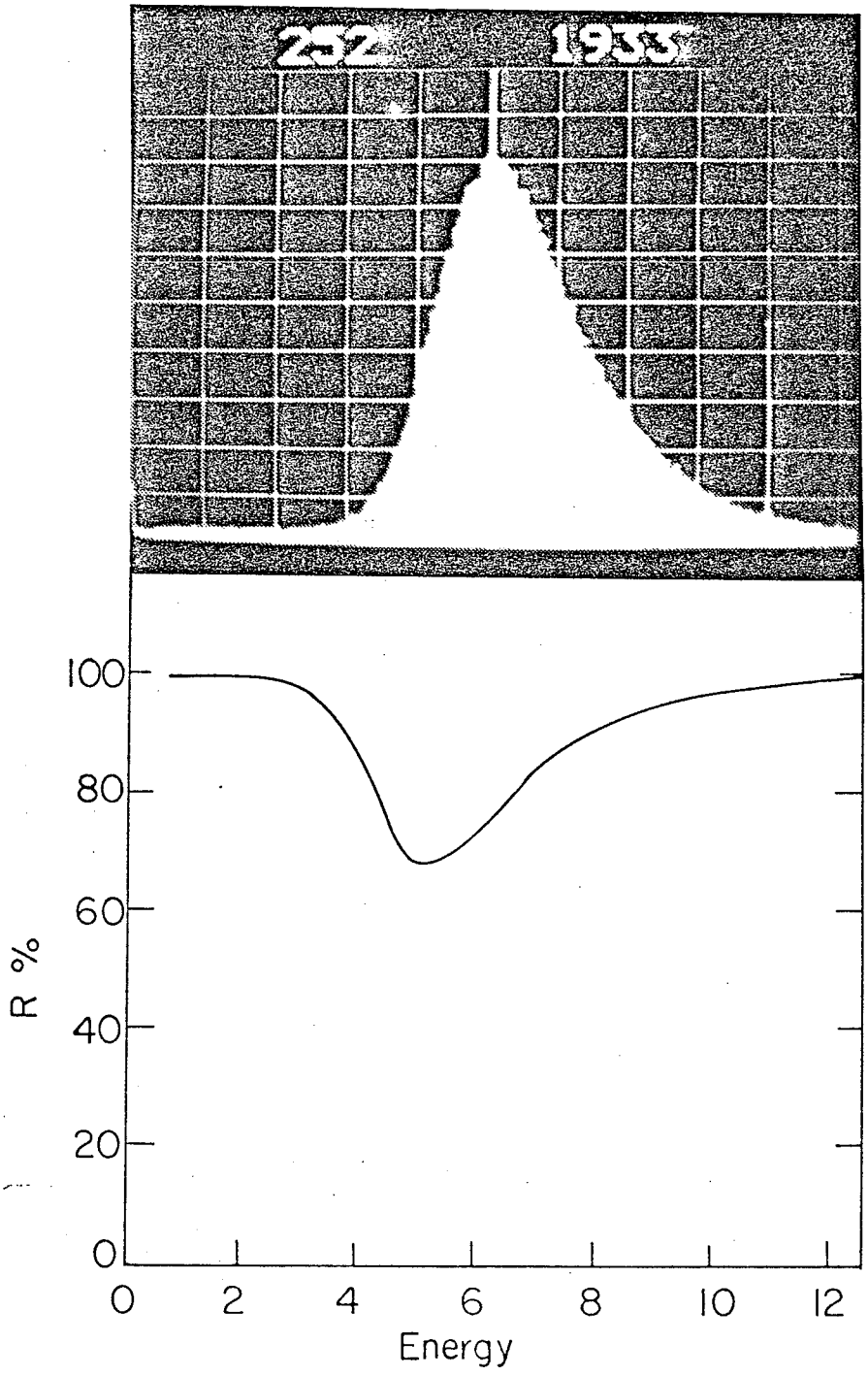

Fig. 15